

ASC Report No. 15/2010

# **Analysis of a Bipolar Energy-Transport Model for a Metal-Oxide-Semiconductor Diode**

Ansgar Jüngel, René Pinnau, Elisa Röhrig

Institute for Analysis and Scientific Computing  
Vienna University of Technology — TU Wien  
[www.asc.tuwien.ac.at](http://www.asc.tuwien.ac.at) ISBN 978-3-902627-03-2

## Most recent ASC Reports

- 14/2010 *Markus Aurada, Michael Ebner, Michael Feischl, Samuel Ferraz-Leite, Petra Goldenits, Michael Karkulik, Markus Mayr, Dirk Praetorius*  
Hilbert (Release 2): A MATLAB Implementation of Adaptive BEM
- 13/2010 *Alexander Dick, Othmar Koch, Roswitha März, Ewa Weinmüller*  
Convergence of Collocation Schemes for Nonlinear Index 1 DAEs with a Singular Point
- 12/2010 *Markus Aurada, Samuel Ferraz-Leite, Petra Goldenits, Michael Karkulik, Markus Mayr, Dirk Praetorius*  
Convergence of Adaptive BEM for some Mixed Boundary Value Problem
- 11/2010 *Mario Bukal, Ansgar Jüngel, Daniel Matthes*  
Entropies for Radially Symmetric Higher-Order Nonlinear Diffusion Equations
- 10/2010 *Karl Rupp, Ansgar Jüngel, Karl-Tibor Grasser*  
Matrix Compression for Spherical Harmonics Expansions of the Boltzmann Transport Equation for Semiconductors
- 9/2010 *Markus Aurada, Samuel Ferraz-Leite, Dirk Praetorius*  
Estimator Reduction and Convergence of Adaptive BEM
- 8/2010 *Robert Hammerling, Othmar Koch, Christa Simon, Ewa B. Weinmüller*  
Numerical Solution of singular Eigenvalue Problems for ODEs with a Focus on Problems Posed on Semi-Infinite Intervals
- 7/2010 *Robert Hammerling, Othmar Koch, Christa Simon, Ewa B. Weinmüller*  
Numerical Solution of Singular ODE Eigenvalue Problems in Electronic Structure Computations
- 6/2010 *Markus Aurada, Michael Feischl, Dirk Praetorius*  
Convergence of Some Adaptive FEM-BEM Coupling
- 5/2010 *Marcus Page, Dirk Praetorius*  
Convergence of Adaptive FEM for some Elliptic Obstacle Problem

Institute for Analysis and Scientific Computing  
Vienna University of Technology  
Wiedner Hauptstraße 8–10  
1040 Wien, Austria

**E-Mail:** [admin@asc.tuwien.ac.at](mailto:admin@asc.tuwien.ac.at)  
**WWW:** <http://www.asc.tuwien.ac.at>  
**FAX:** +43-1-58801-10196

ISBN 978-3-902627-03-2

© Alle Rechte vorbehalten. Nachdruck nur mit Genehmigung des Autors.



# ANALYSIS OF A BIPOLAR ENERGY-TRANSPORT MODEL FOR A METAL-OXIDE-SEMICONDUCTOR DIODE

ANSGAR JÜNGEL, RENÉ PINNAU, AND ELISA RÖHRIG

ABSTRACT. A simplified bipolar energy-transport model for a metal-oxide-semiconductor diode (MOS) with nonconstant lattice temperature is considered. The particle current densities vanish in the diode but the particle temperatures may be large. The existence of weak solutions to the system of quasilinear elliptic equations with nonlinear boundary conditions is proved using a Stampacchia truncation technique and maximum principle arguments. Further, an asymptotic analysis for the one-dimensional MOS diode is presented, which shows that only the boundary temperature influences the capacitance-voltage characteristics of the device. The analytical results are underlined by numerical experiments.

**AMS Classification.** 35J65, 35D05, 35B40, 82D37.

**Keywords.** MOS diode, energy-transport model, electron temperature, lattice temperature, existence of weak solutions, asymptotic analysis, numerics, device characteristics.

## 1. INTRODUCTION

MOS (metal-oxide-semiconductor) diodes are important devices in solid-state electronics [10]. They are utilized as voltage-dependent capacitors, charge-coupled devices, and photo detectors. Another application is their use in on-chip temperature sensors [11]. Usually, MOS diode models are based on the drift-diffusion equations [8, 9] or, in the case of MOS tunneling diodes, on the quantum drift-diffusion equations [15, 16].

In this paper, we analyze and approximate numerically a MOS diode model including thermal effects. For this aim, we propose a stationary bipolar energy-transport model for the particle densities and the particle temperatures, coupled to the Poisson equation for the electric potential and to a heat equation for the lattice temperature. Since there is no current flow in a MOS diode, the energy-transport model can be reduced, under some assumptions detailed in Section 2, to the following system of equations:

$$\begin{aligned}
 (1) \quad & \lambda^2 \operatorname{div}(T \nabla \log n) = n - p - 1, \\
 (2) \quad & \lambda^2 \operatorname{div}(T \nabla \log p) = -(n - p - 1), \\
 (3) \quad & \lambda^2 \Delta V = n - p - 1, \\
 (4) \quad & \operatorname{div}((n + p) \nabla T) = \frac{2}{3\mu_n} W_n(n, T, T_L) + \frac{2}{3\mu_p} W_p(p, T, T_L), \\
 (5) \quad & \operatorname{div}(\kappa \nabla T_L) = -(W_n(n, T, T_L) + W_p(p, T, T_L)).
 \end{aligned}$$

---

The first author acknowledges partial support from the Austrian Science Fund (FWF), grant P20214 and WK “Differential Equations” and from the Austrian Exchange Service (ÖAD), grants ES 08/2010, FR 07/2010, and HR 01/2010. The second author acknowledges support from the German Science Foundation (DFG), grant PI 408/5, as well as grant PI 408/7 in the framework of the Priority Program 1253.

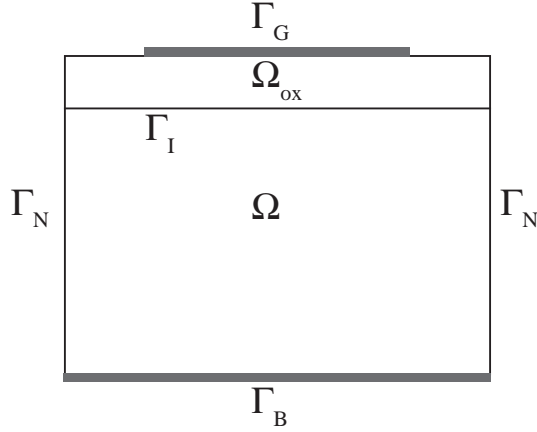


FIGURE 1. Geometry of the MOS diode.

The unknowns are the electron and hole densities  $n$  and  $p$ , the particle and lattice temperatures  $T$  and  $T_L$ , respectively, and the electric potential  $V$ . The scaled physical parameters are the Debye length  $\lambda$ , the electron and hole mobilities  $\mu_n$  and  $\mu_p$ , respectively, and the heat conductivity  $\kappa(x)$ . The energy relaxation terms are given by

$$(6) \quad W_n(n, T, T_L) = \frac{3}{2} \frac{n(T - T_L)}{\tau_n}, \quad W_p(p, T, T_L) = \frac{3}{2} \frac{p(T - T_L)}{\tau_p},$$

where  $\tau_n$  and  $\tau_p$  are the relaxation times.

Equations (1)-(5) are solved in the semiconductor domain  $\Omega \subset \mathbb{R}^d$  ( $d \in \mathbb{N}$ ). In the oxide region  $\Omega_{\text{ox}}$ , we assume that  $\Delta V = 0$ . The domain boundary consists of an insulating part  $\Gamma_N$ , the bulk contact  $\Gamma_B$ , the gate contact near the oxide  $\Gamma_G$ , and the interface  $\Gamma_I$  between the oxide and the semiconductor, i.e.,  $\Gamma_I = \overline{\Omega} \cap \overline{\Omega_{\text{ox}}}$  (see Figure 1). In Section 2 the following boundary conditions are motivated:

$$(7) \quad \nabla n \cdot \nu = \nabla p \cdot \nu = \nabla T \cdot \nu = \nabla T_L \cdot \nu = \nabla V \cdot \nu = 0 \quad \text{on } \Gamma_N,$$

$$(8) \quad V = V_D \quad \text{on } \Gamma_B \cup \Gamma_G,$$

$$(9) \quad n = \delta e^{V/T_D}, \quad p = \delta e^{-V/T_D}, \quad T = T_D, \quad T_L = T_D \quad \text{on } \Gamma_B \cup \Gamma_I,$$

where  $\delta$  is the intrinsic density,  $\nu$  the exterior unit normal on the boundary,  $V_D$  the boundary potential, and  $T_D$  the boundary temperature. Notice that the boundary condition for  $n$  and  $p$  on  $\Gamma_I$  involve the unknown potential  $V$  and are therefore nonlinear.

Adding equations (1) and (2) for the particle densities leads to  $\text{div}(T \nabla \log(np)) = 0$  in  $\Omega$  with the boundary conditions  $\nabla \log(np) \cdot \nu = 0$  on  $\Gamma_N$  and  $\log(np) = \log(\delta^2)$  on  $\Gamma_B \cup \Gamma_I$ . Therefore, the particle densities are related by  $np = \delta^2$ , and one of the equations (1) or (2) can be dropped.

In this paper, we derive the simplified model equations in Section 2 and prove the existence of weak solutions to the above nonlinear boundary-value problem in Section 3 by means of Stampacchia's truncation technique and maximum principle arguments, assuming that  $\delta > 0$  is sufficiently small. Further, we perform in Section 4 an asymptotic analysis (for  $\lambda \rightarrow 0$ ) of the one-dimensional model for the MOS diode and present finally, in Section 5, some numerical tests underlining our analytical results.

## 2. MODELING

We consider the following (scaled) stationary bipolar energy-transport model taken from [2]:

$$(10) \quad \operatorname{div} J_n = R(n, p), \quad J_n = \nabla(\tilde{\mu}_n(T_L)T_L n) - \tilde{\mu}_n(T_L)T_L \frac{n}{T_n} \nabla V,$$

$$(11) \quad \operatorname{div} J_p = R(n, p), \quad J_p = \nabla(\tilde{\mu}_p(T_L)T_L p) + \tilde{\mu}_p(T_L)T_L \frac{p}{T_p} \nabla V,$$

$$(12) \quad \operatorname{div} S_n = \nabla V \cdot J_n + W_n(n, T_n, T_L) + \frac{3}{2}T_n R(n, p),$$

$$(13) \quad S_n = \nabla\left(\frac{3}{2}\tilde{\mu}_n(T_L)T_L T_n n\right) - \frac{3}{2}\tilde{\mu}_n(T_L)T_L n \nabla V,$$

$$(14) \quad \operatorname{div} S_p = -\nabla V \cdot J_p + W_p(p, T_p, T_L) + \frac{3}{2}T_p R(n, p),$$

$$(15) \quad S_p = \nabla\left(\frac{3}{2}\tilde{\mu}_p(T_L)T_L T_p p\right) + \frac{3}{2}\tilde{\mu}_p(T_L)T_L p \nabla V,$$

$$(16) \quad \lambda^2 \Delta V = n - p - C(x),$$

where  $T_n$  and  $T_p$  are the electron and hole temperatures, respectively,  $S_n$  and  $S_p$  are the energy fluxes,  $\tilde{\mu}_n$  and  $\tilde{\mu}_p$  are the temperature-dependent mobility functions,  $C(x)$  is the doping concentration, and the Shockley-Read-Hall recombination-generation term is given by

$$R(n, p) = \frac{np - \delta^2}{\tau_0(n, p)},$$

where  $\tau_0(n, p)$  is some positive function. The energy-transport equations are coupled to the Poisson equation (3) and to the heat equation

$$(17) \quad \operatorname{div}(\kappa \nabla T_L) = -(W_n + W_p) - R(n, p) \left( E_g + \frac{3}{2}(T_n + T_p) \right),$$

where  $E_g > 0$  is the energy gap of the semiconductor material.

The energy-transport equations can be derived from the semiconductor Boltzmann equation in the diffusion limit [1]. The above model corresponds to the so-called Chen model, which is characterized by a special choice for the elastic collision rate (see [7] for details). The heat equation for the lattice temperature follows from thermodynamic principles, neglecting radiation effects and the space dependency of the energy band; see, e.g., [2, Formula (9)] and [14].

For the analysis of the above model, we impose some simplifying assumptions. First, we assume that

$$\tilde{\mu}_n(T_L) = \frac{\mu_n}{T_L}, \quad \tilde{\mu}_p(T_L) = \frac{\mu_p}{T_L},$$

where  $\mu_n, \mu_p > 0$ .

**Remark 1.** In the physical literature, the electron mobility is often given by  $\tilde{\mu}_n(T_L) = \mu_n/T_L^\alpha$ , where  $\alpha$  lies in between 1.5 and 2.3 depending on the semiconductor material and the temperature range [5]. The above assumption still takes into account that the mobility decreases as the temperature increases. The special choice of  $\alpha = 1$  simplifies our analysis.

Second, we suppose that the scaled intrinsic density  $\delta$  is independent of the lattice temperature. This condition is approximately satisfied if the lattice temperature variations are not too large.

The third assumption is that there is no current flow,  $J_n = J_p = 0$  in  $\Omega$ , and the doping concentration is constant,  $C(x) = 1$ . These conditions are natural for a MOS diode and they are also employed in, e.g., [9]. Then equations (10) and (11) reduce to  $R(n, p) = 0$  or  $np = \delta^2$  and

$$(18) \quad T_n \nabla \log n = \nabla V \quad \text{and} \quad T_p \nabla \log p = -\nabla V \quad \text{in } \Omega.$$

Since  $np = \delta^2$  implies that  $\nabla \log n + \nabla \log p = 0$ , the sum of the above equations yields

$$(T_n - T_p) \nabla \log n = 0.$$

Clearly, this does not imply that  $T_n = T_p$  in  $\Omega$ . However, both temperatures coincide in domains in which  $n$  is not constant. This motivates the fourth assumption

$$T_n = T_p = T.$$

Since the particle temperatures are mainly influenced by the lattice temperature, this assumption seems to be reasonable. We remark that also for the general energy-transport model in [3], a common particle temperature for all species was considered.

With the above assumptions, we can simplify the nonisothermal energy-transport model. The equations in (18) give

$$\lambda^2 \operatorname{div}(T \nabla \log n) = \lambda^2 \Delta V = n - p - 1, \quad \lambda^2 \operatorname{div}(T \nabla \log p) = -(n - p - 1),$$

which equal (1) and (2). In view of (18), equations (12)-(13) and (14)-(15) simplify to

$$\frac{3}{2} \mu_n \operatorname{div}(n \nabla T) = W_n(n, T, T_L), \quad \frac{3}{2} \mu_p \operatorname{div}(p \nabla T) = W_p(p, T, T_L),$$

whose sum is (4). Finally, the heat equation (17) becomes

$$\operatorname{div}(\kappa \nabla T_L) = -(W_n + W_p).$$

As explained in the introduction, the boundary of  $\Omega^* = \Omega \cup \Omega_{\text{ox}}$  is assumed to consist of an insulating part  $\Gamma_N$ , the bulk contact  $\Gamma_B$ , and the gate contact  $\Gamma_G$ . Furthermore, we set  $\Gamma_I = \bar{\Omega} \cap \bar{\Omega}_{\text{ox}}$ , the interface between the semiconductor and the oxide part. We assume no-flux boundary conditions at the insulating boundary, which gives (7). The electric potential is assumed to be given at the gate and bulk contacts, which is (8). We suppose that, on  $\Gamma_B \cup \Gamma_I$ , the particle temperature is equal to the lattice temperature and that  $T_L$  is constant on each boundary segment,  $T = T_L = T_D$  on  $\Gamma_B$  and  $T = T_L = T_D$  on  $\Gamma_I$ . Then (18) can be integrated on the boundary,  $\log n - V/T_D = \text{const.}$  on  $\Gamma_B$  and  $\log n - V/T_D = \text{const.}$  on  $\Gamma_I$ . Because of (18), the constants coincide and can be fixed by defining a reference point for the electric potential,  $\log n - V/T_D = \log \delta$ . This implies that

$$n = \delta e^{V/T_D} \quad \text{and} \quad p = \delta e^{-V/T_D} \quad \text{on } \Gamma_B \cup \Gamma_I.$$

It is convenient to introduce the variable  $u$  by  $n = \delta e^u$ . Then  $p = \delta e^{-u}$  and equations (1)-(9) become

$$(19) \quad \lambda^2 \operatorname{div}(T \nabla u) = 2\delta \sinh u - 1,$$

$$(20) \quad \lambda^2 \Delta V = 2\delta \sinh u - 1,$$

$$(21) \quad \operatorname{div}(\cosh u \nabla T) = \frac{1}{2} \left( \frac{e^u}{\mu_n \tau_n} + \frac{e^{-u}}{\mu_p \tau_p} \right) (T - T_L),$$

$$(22) \quad \operatorname{div}(\kappa \nabla T_L) = -\frac{3\delta}{2} \left( \frac{e^u}{\tau_n} + \frac{e^{-u}}{\tau_p} \right) (T - T_L) \quad \text{in } \Omega,$$

as well as  $\Delta V = 0$  in  $\Omega_{\text{ox}}$ . The boundary conditions read as

$$(23) \quad \nabla u \cdot \nu = \nabla T \cdot \nu = \nabla T_L \cdot \nu = \nabla V \cdot \nu = 0 \quad \text{on } \Gamma_N,$$

$$(24) \quad V = V_D \quad \text{on } \Gamma_B \cup \Gamma_G,$$

$$(25) \quad u = V/T_D, \quad T = T_D, \quad T_L = T_D \quad \text{on } \Gamma_B \cup \Gamma_I.$$

Clearly, every bounded weak solution to (19)-(25) provides a solution to (1)-(9) via  $n = \delta e^u$  and  $p = \delta e^{-u}$ .

**Remark 2.** The above model is designed in such a way that in thermal equilibrium ( $T_D|_{\Gamma_B} = T_D|_{\Gamma_I} = \text{const.}$ ), a solution to the above system is given by  $T = T_L = T_D$ ,  $n = \delta e^{V/T_D}$ ,  $p = \delta e^{-V/T_D}$  in  $\Omega$ , and  $V$  is the unique solution to

$$\begin{aligned} \lambda^2 \Delta V &= 2\delta \sinh V - 1 \quad \text{in } \Omega, \quad \Delta V = 0 \quad \text{in } \Omega_{\text{ox}}, \\ V &= V_D \quad \text{on } \Gamma_B \cup \Gamma_G, \quad \nabla V \cdot \nu = 0 \quad \text{on } \Gamma_N. \end{aligned}$$

Thus, our model is consistent with the thermal equilibrium state for the temperature independent standard drift-diffusion model [9].

### 3. EXISTENCE ANALYSIS

This section is devoted to the proof of the existence of solutions to the boundary-value problem (19)-(25). For the proof we use a Stampacchia truncation method and a fixed-point argument. We consider first the following truncated system:

$$(26) \quad \lambda^2 \operatorname{div}([T] \nabla u) = 2\delta \sinh[u] - 1,$$

$$(27) \quad \lambda^2 \Delta V = 2\delta \sinh[u] - 1,$$

$$(28) \quad \operatorname{div}(\cosh[u] \nabla T) = \left( \frac{e^{[u]}}{\mu_n \tau_n} + \frac{e^{-[u]}}{\mu_p \tau_p} \right) (T - [T_L]),$$

$$(29) \quad \operatorname{div}(\kappa \nabla T_L) = -\frac{3\delta}{2} \left( \frac{e^{[u]}}{\tau_n} + \frac{e^{-[u]}}{\tau_p} \right) ([T] - T_L) \quad \text{in } \Omega,$$

and  $\Delta V = 0$  in  $\Omega_{\text{ox}}$ , where

$$\begin{aligned} [T] &= \min\{T_0, \max\{T_1, T\}\}, \\ [T_L] &= \min\{T_0, \max\{T_1, T_L\}\}, \\ [u] &= \min\{u_0, \max\{u_1, u\}\}. \end{aligned}$$

The constants are defined by

$$(30) \quad \begin{aligned} T_0 &= \inf_{\Gamma_B \cup \Gamma_I} T_D, & T_1 &= \sup_{\Gamma_B \cup \Gamma_I} T_D, \\ V_0 &= \inf_{\Gamma_B \cup \Gamma_G} V_D, & V_1 &= \sup_{\Gamma_B \cup \Gamma_G} V_D, \\ u_0 &= \min \left\{ \frac{V_0}{T_0}, \frac{V_0}{T_1} \right\}, & u_1 &= \sinh^{-1} \left( \frac{1}{2\delta} \right). \end{aligned}$$

In order to ensure that  $u_0 \leq u_1$ , we let  $\delta_0 > 0$  be such that

$$(31) \quad \min \left\{ \frac{V_0}{T_0}, \frac{V_0}{T_1} \right\} \leq \sinh^{-1} \left( \frac{1}{2\delta_0} \right),$$

and we choose  $0 < \delta \leq \delta_0$ .

We are able to deduce a priori estimates if the scaled intrinsic density  $\delta$  is sufficiently small. The scaled intrinsic density  $\delta$  is the quotient of the physical intrinsic density  $n_i$  and

the maximal doping concentration  $C_M$ . Since typically,  $n_i$  is of the order  $10^{10} \text{ cm}^{-3}$  and  $C_M$  is of the order  $10^{16} \text{ cm}^{-3}$ , we have  $\delta \approx 10^{-6}$ . Thus, in applications,  $\delta$  is indeed a small parameter (compared to one). In particular, since  $V$  and  $T$  are of order one in the scaled model, condition (31) is satisfied.

**Lemma 3.** *Let  $0 < \kappa_0 \leq \kappa(x) \leq \kappa_1$  for  $x \in \Omega$  and let  $(u, T, T_L, V) \in H^1(\Omega)^3 \times H^1(\Omega^*)$  be a weak solution to (26)-(29) with boundary conditions (23)-(25). Then there exist  $\delta_0 > 0$  and  $c > 0$  such that for all  $0 < \delta \leq \delta_0$ ,*

$$\begin{aligned} T_0 \leq T, T_L \leq T_1, \quad u_0 \leq u \leq u_1 \quad \text{in } \Omega, \quad V_0 \leq V \leq \bar{V}_\delta \quad \text{in } \Omega^*, \\ \|u\|_{H^1(\Omega)} + \|T\|_{H^1(\Omega)} + \|T_L\|_{H^1(\Omega)} + \|V\|_{H^1(\Omega^*)} \leq c. \end{aligned}$$

The lower and upper bounds are defined in (30) and  $\bar{V}_\delta$  is defined in (32).

*Proof.* We set in the following  $z^+ = \max\{0, z\}$  and  $z^- = \min\{0, z\}$  for  $z \in \mathbb{R}$ .

*Step 1:* Lower and upper bounds for  $T$  and  $T_L$ . The test function  $(T - T_1)^+$  is admissible in the weak formulation of (28) since  $(T - T_1)^+ = (T_D - T_1)^+ = 0$  on  $\Gamma_B \cup \Gamma_I$ , by the definition of  $T_1$ . Then, since  $\cosh[u] \geq 1$ ,

$$\begin{aligned} \int_{\Omega} |\nabla(T - T_1)^+|^2 dx &\leq -\frac{1}{2} \int_{\Omega} \left( \frac{e^{[u]}}{\mu_n \tau_n} + \frac{e^{-[u]}}{\mu_p \tau_p} \right) (T - [T_L]) (T - T_1)^+ dx \\ &\leq -\frac{1}{2} \int_{\Omega} \left( \frac{e^{[u]}}{\mu_n \tau_n} + \frac{e^{-[u]}}{\mu_p \tau_p} \right) (T - T_1) (T - T_1)^+ dx \leq 0, \end{aligned}$$

and hence  $T \leq T_1$  in  $\Omega$ . Similarly, using  $(T - T_0)^-$  as an admissible test function, it follows that  $T \geq T_0$  in  $\Omega$ . In an analogous way, we obtain the bounds  $T_0 \leq T_L \leq T_1$  in  $\Omega$ .

*Step 2:* Lower bounds for  $V$  and  $u$ . The test function  $(V - V_0)^-$  in (27) is admissible since it vanishes on  $\Gamma_B \cup \Gamma_G$ . This gives

$$\begin{aligned} \lambda^2 \int_{\Omega^*} |\nabla(V - V_0)^-|^2 dx &= \int_{\Omega} (2\delta \sinh[u] - 1) [-(V - V_0)^-] dx \\ &\leq \int_{\Omega} (2\delta \sinh u_1 - 1) [-(V - V_0)^-] dx = 0, \end{aligned}$$

using the definitions of  $[u]$  and  $u_1$ . This implies that  $V \geq V_0$  in  $\Omega^*$ .

Next, we observe that, on  $\Omega$ ,

$$\frac{V}{T} \geq \inf_{\Omega} \frac{V}{T} \geq \min \left\{ \frac{\inf_{\Omega} V}{\inf_{\Omega} T}, \frac{\inf_{\Omega} V}{\sup_{\Omega} T} \right\} = \min \left\{ \frac{V_0}{T_0}, \frac{V_0}{T_1} \right\} = u_0.$$

This estimate also holds on  $\Gamma_B \cup \Gamma_I$ . Hence,  $(u - u_0)^- = (V/T - u_0)^- = 0$  on  $\Gamma_B \cup \Gamma_I$ , and we can employ this function in the weak formulation of (26):

$$\begin{aligned} \lambda^2 \int_{\Omega} T |\nabla(u - u_0)^-|^2 dx &= \int_{\{u \leq u_0\}} (2\delta \sinh[u] - 1) [-(u - u_0)^-] dx \\ &\leq \int_{\{u \leq u_0\}} (2\delta \sinh u_0 - 1) [-(u - u_0)^-] dx = 0, \end{aligned}$$

since  $2\delta \sinh u_0 \leq 2\delta \sinh u_1 = 1$  by (31). As  $T \geq T_0 > 0$  in  $\Omega$ , we infer that  $u \geq u_0$  in  $\Omega$ .



*Step 3:* Upper bounds for  $V$  and  $u$ . We employ  $(V - V_1)^+$  as (admissible) test function in the weak formulation of (27). Since  $\sinh[u] \geq \sinh u_0$ , we have

$$\begin{aligned} \lambda^2 \int_{\Omega^*} |\nabla(V - V_1)^+|^2 dx &= \int_{\Omega^*} (1 - 2\delta \sinh[u])(V - V_1)^+ dx \\ &\leq (1 - 2\delta \sinh u_0) \int_{\Omega^*} (V - V_1)^+ dx \\ &\leq c_p(1 - 2\delta \sinh u_0) \|\nabla(V - V_1)^+\|_{L^2(\Omega^*)} (\text{meas}(V > V_1))^{1/2}, \end{aligned}$$

where  $c_p > 0$  is the Poincaré constant. Let  $r > 2$  be such that the embedding  $H^1(\Omega^*) \hookrightarrow L^r(\Omega^*)$  is continuous. It is well known [12, Chap. 4] that for  $W > V_1$ , it holds

$$(\text{meas}(V > W))^{1/r} (W - V_1) \leq c(\Omega^*, d) \|\nabla(V - V_1)^+\|_{L^2(\Omega^*)},$$

where  $c(\Omega^*, d) > 0$  is a constant only depending on  $\Omega^*$  and  $d$ . Thus

$$\text{meas}(V > W) \leq (c(\Omega^*, d) c_p \lambda^{-2} (1 - 2\delta \sinh u_0))^r \frac{(\text{meas}(V > V_1))^{r/2}}{(W - V_1)^r}.$$

Since  $r/2 > 1$ , we can apply Stampacchia's lemma (see [12, Chap. 4] or [13, Lemma 2.9]) to conclude that  $V \leq \bar{V}_\delta$  in  $\Omega^*$ , where

$$(32) \quad \bar{V}_\delta = V_1 + c(\Omega^*, d) c_p \lambda^{-2} (1 - 2\delta \sinh u_0).$$

We impose a second condition on the choice of  $\delta_0$  (and  $\delta$ ):

$$(33) \quad \max \left\{ \frac{\bar{V}_{\delta_0}}{T_0}, \frac{\bar{V}_{\delta_0}}{T_1} \right\} \leq \sinh^{-1} \left( \frac{1}{2\delta_0} \right).$$

Such a  $\delta_0$  exists since  $\bar{V}_{\delta_0}$  is bounded as  $\delta_0 \rightarrow 0$ , whereas  $\sinh^{-1}(1/2\delta_0)$  tends to  $+\infty$  as  $\delta_0 \rightarrow 0$ . This inequality also holds for all  $\delta \leq \delta_0$ . Hence, on  $\Omega$ ,

$$\frac{V}{T} \leq \sup_{\Omega} \frac{V}{T} \leq \max \left\{ \frac{\sup_{\Omega} V}{\inf_{\Omega} T}, \frac{\sup_{\Omega} V}{\sup_{\Omega} T} \right\} \leq \max \left\{ \frac{\bar{V}_\delta}{T_0}, \frac{\bar{V}_\delta}{T_1} \right\} \leq \sinh^{-1} \left( \frac{1}{2\delta} \right) = u_1.$$

This inequality holds true on  $\Gamma_B \cup \Gamma_I$  as well such that

$$(u - u_1)^+ = \left( \frac{V}{T} - u_1 \right)^+ = 0 \quad \text{on } \Gamma_B \cup \Gamma_I.$$

As a consequence, the test function  $(u - u_1)^+$  is admissible in (26) and we obtain

$$\begin{aligned} \lambda^2 \int_{\Omega} T |\nabla(u - u_1)^+|^2 dx &= \int_{\{u \geq u_1\}} (1 - 2\delta \sinh[u])(u - u_1)^+ dx \\ &= \int_{\{u \geq u_1\}} (1 - 2\delta \sinh u_1)(u - u_1)^+ dx = 0, \end{aligned}$$

by the definition of  $u_1$ . We conclude that  $u \leq u_1$  in  $\Omega$ .

*Step 4:*  $H^1$  estimates. In view of the  $L^\infty$  estimates for  $T$  and  $T_L$ , the  $H^1$  bounds for  $T$  and  $T_L$  follow immediately after employing  $T - T_D$  and  $T_L - T_D$  as test functions in (28) and (29), respectively. The right-hand side of the Poisson equation (27) is bounded in  $\Omega^*$ ; therefore,  $V$  can be bounded in  $H^1(\Omega)$  and the bound depends on the  $L^\infty$  bound for  $u$  and the  $H^1$  bound for  $V_D$ . The same argument applies to  $u$ .  $\square$

**Theorem 4** (Existence of solutions). *Let  $\lambda, \mu_i, \tau_i > 0$  ( $i = n, p$ ),  $0 < \kappa_0 \leq \kappa(x) \leq \kappa_1$  for  $x \in \Omega$ , and  $V_D \in H^1(\Omega^*) \cap L^\infty(\Omega^*)$ ,  $T_D \in H^1(\Omega) \cap L^\infty(\Omega)$ . Furthermore, let  $0 < \delta \leq \delta_0$ , where  $\delta_0$  is defined in (31) and (33). Then there exists a weak solution  $(u, T, T_L) \in (H^1(\Omega) \cap L^\infty(\Omega))^3$ ,  $V \in H^1(\Omega^*) \cap L^\infty(\Omega^*)$  to (19)-(25).*

*Proof.* The proof is based on the Leray-Schauder fixed-point theorem [4]. For the definition of the fixed-point operator, let  $w \in L^2(\Omega)$  and  $\sigma \in [0, 1]$ . Then, let  $V \in H^1(\Omega) \cap L^\infty(\Omega)$  be the unique solution to the linear problem

$$\begin{aligned} \lambda^2 \Delta V &= 2\delta \sinh[w] - 1 \quad \text{in } \Omega, \quad \Delta V = 0 \quad \text{in } \Omega_{\text{ox}}, \\ \nabla V \cdot \nu &= 0 \quad \text{on } \Gamma_N, \quad V = V_D \quad \text{on } \Gamma_B \cup \Gamma_G; \end{aligned}$$

let  $T_L \in H^1(\Omega)$  be the unique solution to the linear problem

$$\begin{aligned} \operatorname{div}(\kappa \nabla T_L) &= -\frac{3\delta}{2} \left( \frac{e^{[w]}}{\tau_n} + \frac{e^{-[w]}}{\tau_p} \right) (T - [T_L]) \quad \text{in } \Omega, \\ \nabla T_L \cdot \nu &= 0 \quad \text{on } \Gamma_N, \quad T_L = T_D \quad \text{on } \Gamma_B \cup \Gamma_I; \end{aligned}$$

and let  $T \in H^1(\Omega)$  be the unique solution to

$$\begin{aligned} \operatorname{div}(\cosh[w] \nabla T) &= \frac{\sigma}{2} \left( \frac{e^{[w]}}{\mu_n \tau_n} + \frac{e^{-[w]}}{\mu_p \tau_p} \right) (T - [T_L]) \quad \text{in } \Omega, \\ \nabla T \cdot \nu &= 0 \quad \text{on } \Gamma_N, \quad T = \sigma T_D \quad \text{on } \Gamma_B \cup \Gamma_I. \end{aligned}$$

Finally, let  $u \in H^1(\Omega)$  be the unique solution to

$$\begin{aligned} \lambda^2 \operatorname{div}([T] \nabla u) &= \sigma (2\delta \sinh[w] - 1) \quad \text{in } \Omega, \\ \nabla u \cdot \nu &= 0 \quad \text{on } \Gamma_N, \quad u = \sigma V / T_D \quad \text{on } \Gamma_B \cup \Gamma_G. \end{aligned}$$

This defines the fixed-point operator  $S : L^2(\Omega) \times [0, 1] \rightarrow L^2(\Omega)$ ,  $S(w, \sigma) = u$ . Clearly,  $S(w, 0) = 0$ . Furthermore, by standard arguments,  $S$  is continuous and, since  $u$  lies in  $H^1(\Omega)$  which embeds compactly into  $L^2(\Omega)$ , also compact. Lemma 3 provides uniform  $H^1(\Omega)$  bounds for  $u$ . In fact, Lemma 3 only settles the case  $\sigma = 1$  but the proof for  $\sigma \leq 1$  is similar. Thus, by the Leray-Schauder theorem, we conclude the existence of a fixed point of  $S(\cdot, 1)$ , i.e., a solution to (19)-(25).  $\square$

#### 4. ASYMPTOTIC ANALYSIS

Next, we investigate the model (19)-(25) using asymptotic analysis in one spatial dimension. In particular, we want to study the influence of the boundary temperature on the capacitance-voltage characteristics of the MOS diode depicted in Figure 1. The simple device geometry allows for the restriction to one space dimension, such that the model equations stated on  $\Omega = (0, 1)$  simplify to

$$(34) \quad \lambda^2 \partial_x (T \partial_x u) = 2\delta \sinh u - 1,$$

$$(35) \quad \lambda^2 \partial_{xx} V = 2\delta \sinh u - 1,$$

$$(36) \quad \partial_x (\cosh u \partial_x T) = \frac{1}{2} \left( \frac{e^u}{\mu_n \tau_n} + \frac{e^{-u}}{\mu_p \tau_p} \right) (T - T_L),$$

$$(37) \quad \partial_{xx} T_L = -\frac{3\delta}{2} \left( \frac{e^u}{\tau_n} + \frac{e^{-u}}{\tau_p} \right) (T - T_L),$$

where we assumed for notational simplicity that  $\kappa \equiv 1$ . Since  $\partial_{xx}V = 0$  in  $\Omega_{\text{ox}} = (-d, 0)$ ,  $V$  is linear,  $V(x) = \partial_x V(0)x + V(0)$  for  $x \in [-d, 0]$ . The choice  $x = -d$  leads to the Robin boundary condition

$$(38) \quad d\partial_x V(0) = V(0) - V_D(-d)$$

at  $x = 0$ . Hence, it is sufficient to consider the Poisson equation on the interval  $(0, 1)$  only, with the boundary conditions  $V(1) = V_D(1)$  and (38). The other boundary conditions reduce to

$$(39) \quad u = V/T_D, \quad T = T_D, \quad T_L = T_D \quad \text{on } \{0, 1\}.$$

The potential is defined up to an additive constant only; hence, we may choose  $V_D(1) = T_D(1) \sinh^{-1}(1/2\delta)$  and  $V_D(-d) = T_D(1) \sinh^{-1}(1/2\delta) + U$ , where  $U = V_D(-d) - V_D(1)$  is the applied voltage. This yields  $u(1) = V(1)/T_D(1) = \sinh^{-1}(1/2\delta)$ .

We are interested in the behavior of the solution for small  $\lambda$ . First, we consider the reduced problem, which we obtain after setting  $\lambda = 0$  in (34)-(37):

$$\begin{aligned} 2\delta \sinh \bar{u} - 1 &= 0, \quad \partial_x(\bar{T}\partial_x \bar{u} - \partial_x \bar{V}) = 0, \\ \partial_x(\cosh \bar{u} \partial_x \bar{T}) &= \frac{1}{2} \left( \frac{e^{\bar{u}}}{\mu_n \tau_n} + \frac{e^{-\bar{u}}}{\mu_p \tau_p} \right) (\bar{T} - \bar{T}_L), \\ \partial_{xx} \bar{T}_L &= -\frac{3\delta}{2} \left( \frac{e^{\bar{u}}}{\tau_n} + \frac{e^{-\bar{u}}}{\tau_p} \right) (\bar{T} - \bar{T}_L), \quad x \in (0, 1). \end{aligned}$$

The first equation implies that  $\bar{u} = \sinh^{-1}(1/2\delta)$ . Then the second equation, which is obtained from the difference of (34) and (35), implies that  $\bar{V}$  is linear and the choice  $\bar{V} = T_D(1)\bar{u}$  is compatible with the boundary condition  $u = V/T_D$  at  $x = 1$ . Moreover, we may choose  $\bar{T}(x) = \bar{T}_L(x) = T_D(0) + (T_D(1) - T_D(0))x$ , which solves the last two equations as well as the boundary conditions (39).

It is obvious that the reduced solution cannot fulfill all boundary conditions at  $x = 0$ , such that we can expect that a boundary layer will occur. We introduce the scaled layer variable  $\xi = x/\lambda$  and write the variables as  $W(x, \xi, \lambda) = \bar{W}(x) + \hat{W}(\xi) + O(\lambda)$  (as  $\lambda \rightarrow 0$ ). Introducing this ansatz and performing the limit  $\lambda \rightarrow 0$  in (34)-(37) yields the layer problem

$$(40) \quad \partial_\xi((\bar{T}(0) + \hat{T})\partial_\xi \hat{u}) = 2\delta \sinh(\bar{u} + \hat{u}) - 1,$$

$$(41) \quad \partial_{\xi\xi} \hat{V} = 2\delta \sinh(\bar{u} + \hat{u}) - 1,$$

$$(42) \quad \partial_\xi(\cosh(\bar{u} + \hat{u})\partial_\xi \hat{T}) = 0,$$

$$(43) \quad \partial_{\xi\xi} \hat{T}_L = 0, \quad \xi \in (0, \infty).$$

Here, we have used  $\partial_{xx} = \lambda^{-2}\partial_{\xi\xi}$  and  $x = \lambda\xi \rightarrow 0$  as  $\lambda \rightarrow 0$  for fixed  $\xi$ . This system is supplemented with the boundary conditions

$$\begin{aligned} \partial_\xi \hat{V} = 0, \quad \hat{u} = \hat{V}/T_D(0), \quad \hat{T} = 0, \quad \hat{T}_L = 0 \quad \text{at } \xi = 0, \\ \hat{u} = 0, \quad \hat{V} = 0, \quad \hat{T} = 0, \quad \hat{T}_L = 0 \quad \text{for } \xi \rightarrow \infty. \end{aligned}$$

From (42) and (43) together with the above boundary conditions, we immediately deduce that no layer in the temperature occurs, i.e.,  $\hat{T} = \hat{T}_L = 0$ . Hence, we can simplify (40) to

$$T_D(0) \partial_{\xi\xi} \hat{u} = 2\delta \sinh(\bar{u} + \hat{u}) - 1 \quad \text{in } (0, \infty).$$

The boundary conditions allow for the choice  $\hat{u} = \hat{V}/T_D(0)$ , such that the whole layer problem reduces to the solution of

$$\partial_{\xi\xi}\hat{V} = 2\delta \sinh(\bar{u}(0) + \hat{V}/T_D(0)) - 1 \quad \text{in } (0, \infty)$$

supplemented with the boundary conditions

$$\partial_{\xi}\hat{V}(0) = 0, \quad \hat{V}(+\infty) = 0.$$

This layer equation coincides up to the appearance of  $T_D(0)$  with the layer equation derived from the drift-diffusion model (compare [9]). Hence, we obtain the analogous asymptotic device characteristics apart from the scaling factor introduced by the left boundary temperature  $T_D(0)$ . Since the whole device characteristics is determined by the boundary layer for the densities, it is reasonable that only the boundary temperature enters here. This additional factor has the effect that an increase of the left boundary temperature yields a decrease of the overall capacitance of the device and vice versa. Here, the capacitance is defined by  $C = \partial Q/\partial U$ , where  $Q = \int_0^1 (n-p-1)dx$ . These analytical results are underlined by numerical tests which are presented in the next section.

## 5. NUMERICAL APPROXIMATION

In this section we are presenting some numerical results for a one-dimensional MOS diode. We consider the one-dimensional system on the unit interval for different parameter sets. The equations are discretized using standard finite differences on an equidistant grid of 400 points, and the resulting nonlinear systems are solved using a Newton method. In all of the following numerical results we assumed that the (scaled) oxide thickness is  $d = 0.1$  and we choose  $\kappa \equiv 1$ . The mobilities are set to  $\mu_n = 0.14$ ,  $\mu_p = 0.045$  and the relaxation times are given by  $\tau_n = 0.474$  and  $\tau_p = 7.4510^{-4}$ . For the computation of the capacitance-voltage characteristics (CVCs) we use a voltage continuation method, starting from the equilibrium state and increasing the applied voltage step by step. This reduces significantly the number of Newton iterations on each voltage level.

First, we study the current-voltage characteristics of the MOS diode. We are in particular interested in the influence of the boundary temperature. In Figure 2 we present the CVCs for a fixed value of  $\delta = 10^{-3}$  and two values of  $\lambda$ . The right boundary temperature  $T_D(1) = T_1$  is set equal to one and the left boundary temperature  $T_D(0) = T_0$  attains the values 0.9, 1, and 1.1. For  $T_0 = 1$  we obtain the solution of the standard drift-diffusion model. In accordance with our asymptotic analysis in Section 4, we observe that the value  $T_0$  of the left boundary has an influence in the inversion regime only. A larger boundary temperature yields a lower capacitance, while a smaller temperature has the opposite effect.

The influence of the intrinsic density  $\delta$  on the CVC is depicted in Figure 3. Here, we choose  $\lambda = 0.065$ ,  $T_0 = 0.9$  and  $T_1 = 1$ . The behavior is exactly the same as in the drift-diffusion case, where a decrease of  $\delta$  yields an increase of the capacitance in the inversion region.

The state variables, i.e., the electron density (in logarithmic scale), the electrostatic potential, the electron temperature, and the lattice temperature, are depicted in Figure 4 (for  $T_0 = 1$ ) and Figure 5 (for  $T_0 = 0.9$ ), for various applied voltages  $U$ . In both cases, we used the scaled parameters  $\lambda = 0.078$ ,  $\delta = 10^{-3}$ , and  $T_1 = 1$ . The case  $T_0 = T_1 = 1$  in Figure 4 corresponds to the standard drift-diffusion case. In particular, the temperatures are constant in the device. We notice that the electron and the lattice temperature almost coincide, except for large negative values of the applied voltage.

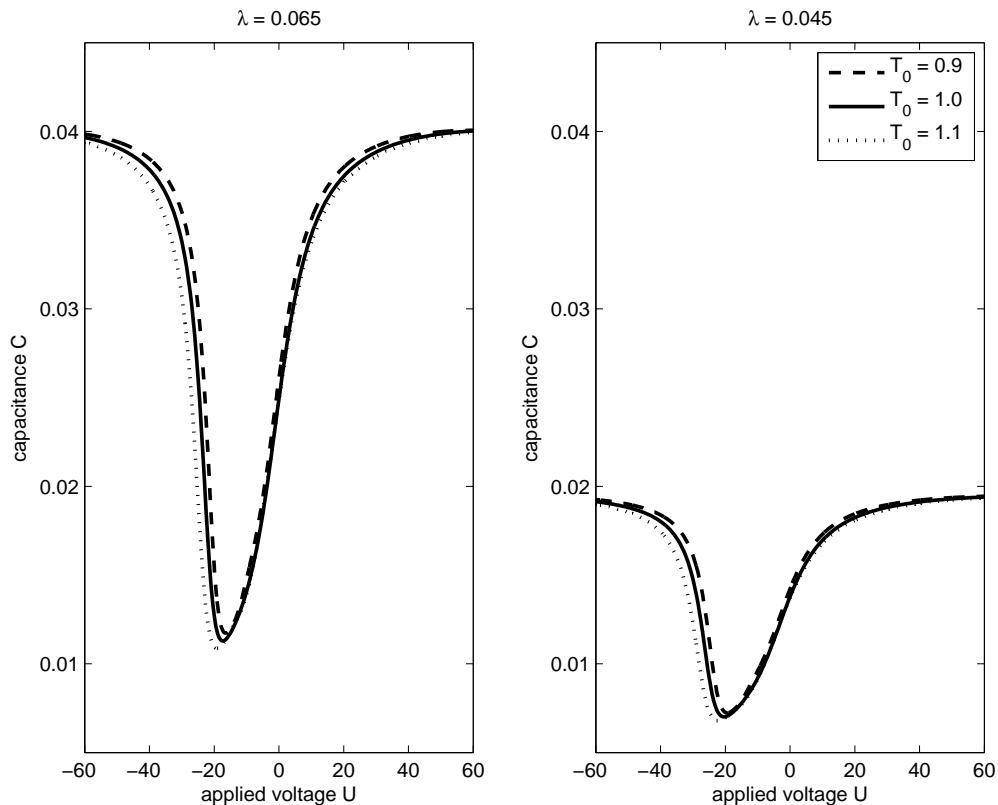


FIGURE 2. Capacitance-voltage characteristics for various values of  $T_0 = T_D(0)$  and  $\lambda$  ( $\delta = 10^{-3}$ ).

## 6. CONCLUSIONS

We presented a new simplified bipolar energy-transport model for a MOS diode with non-constant lattice temperature. The model, consisting of a system of quasilinear elliptic equations with nonlinear boundary conditions, has a weak solution for small values of the intrinsic density. An asymptotic analysis for the one-dimensional MOS diode shows that only the boundary temperature influences the capacitance-voltage characteristics of the MOS diode, which is confirmed by the numerical results.

## REFERENCES

- [1] N. Ben Abdallah and P. Degond. On a hierarchy of macroscopic models for semiconductors. *J. Math. Phys.* 37 (1996), 3308-3333.
- [2] M. Brunk and A. Jüngel. Heating of semiconductor devices in electric circuits. To appear in J. Roos and L. Costa (eds.), *Scientific Computing in Electrical Engineering SCEE 2008*, Mathematics in Industries. Springer, 2010.
- [3] P. Degond, S. Génieys, and A. Jüngel. A system of parabolic equations in nonequilibrium thermodynamics including thermal and electrical effects. *J. Math. Pures Appl.* 76 (1997), 991-1015.
- [4] D. Gilbarg and N. S. Trudinger. *Elliptic Partial Differential Equations of Second Order*. Springer, Berlin, first edition, 1983.
- [5] A. Hasegawa. Mobility change through temperature-dependent mass in semiconductors. *J. Phys. Soc. Japan* 17 (1962), 1402-1404.

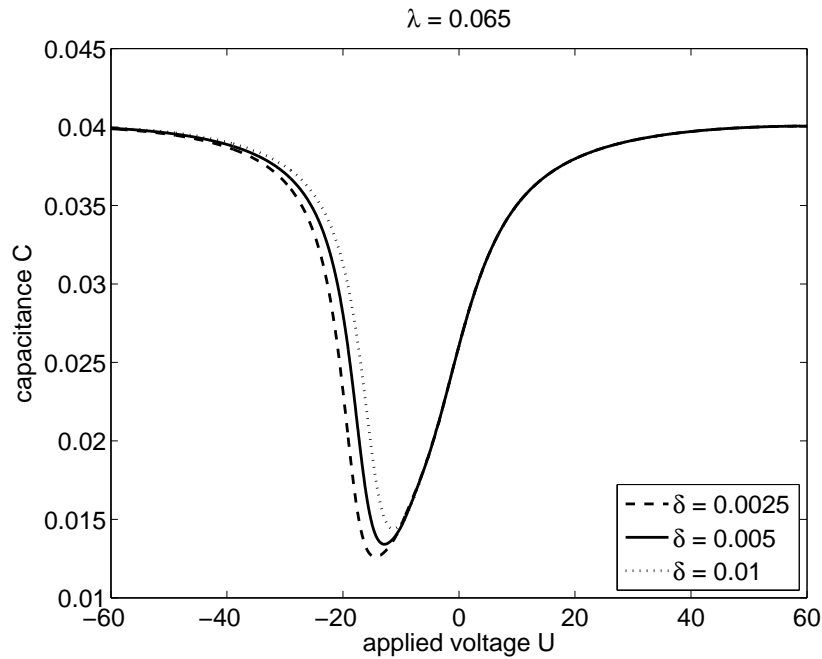


FIGURE 3. Capacitance voltage characteristics for various values of  $\delta$  ( $T_0 = 0.9$ ,  $T_1 = 1$ ).

- [6] A. Jüngel. A steady-state quantum Euler-Poisson system for potential flows. *Commun. Math. Phys.* 194 (1998), 463-479.
- [7] A. Jüngel. *Transport Equations for Semiconductors*. Lecture Notes in Physics 773, Springer, Berlin, 2009.
- [8] P. Markowich, C. Ringhofer, and C. Schmeiser. An asymptotic analysis of one-dimensional models of semiconductor devices. *IMA J. Appl. Math.* 37 (1986), 1-24.
- [9] P. Markowich, C. Ringhofer, and C. Schmeiser. *Semiconductor Equations*. Springer, Vienna, 1990.
- [10] E. Nicollian and J. Brews. *MOS (Metal Oxide Semiconductor) Physics and Technology*. Wiley, New York, 1982.
- [11] Y.-H. Shih and J.-G. Hwu. An on-chip temperature sensor by utilizing a MOS tunneling diode. *IEEE Electron Dev. Lett.* 22 (2001), 299-301.
- [12] G. Stampacchia. *Equations elliptiques du second ordre à coefficients discontinus*. Les Presses de l'Université de Montréal, Canada, 1966.
- [13] G. Troianiello. *Elliptic Differential Equations and Obstacle Problems*. Plenum Press, New York, 1987.
- [14] G. Wachutka. Consistent treatment of carrier emission and capture kinetics in electrothermal and energy transport models. *Microelectr. J.* 26 (1995), 307-315.
- [15] A. Wettstein, *Quantum Effects in MOS Devices*. Hartung-Gorre Verlag, Konstanz, Germany, 2000.
- [16] A. Wettstein, A. Schenk, and W. Fichtner. Quantum device-simulation with the density-gradient model on unstructured grids. *IEEE Trans. Electron Dev.* 48 (2001), 279-284.

INSTITUTE FOR ANALYSIS AND SCIENTIFIC COMPUTING, VIENNA UNIVERSITY OF TECHNOLOGY, WIEDNER HAUPTSTR. 8-10, 1040 WIEN, AUSTRIA; E-MAIL: JUENGL@ANUM.TUWIEN.AC.AT

FACHBEREICH MATHEMATIK, TECHNISCHE UNIVERSITÄT KAISERSLAUTERN, ERWIN-SCHRÖDINGER-STRASSE, 67663 KAISERSLAUTERN, GERMANY; E-MAIL: PINNAU@MATHEMATIK.UNI-KL.DE

FACHBEREICH MATHEMATIK, TECHNISCHE UNIVERSITÄT KAISERSLAUTERN, ERWIN-SCHRÖDINGER-STRASSE, 67663 KAISERSLAUTERN, GERMANY; E-MAIL: ROEHRIG@MATHEMATIK.UNI-KL.DE

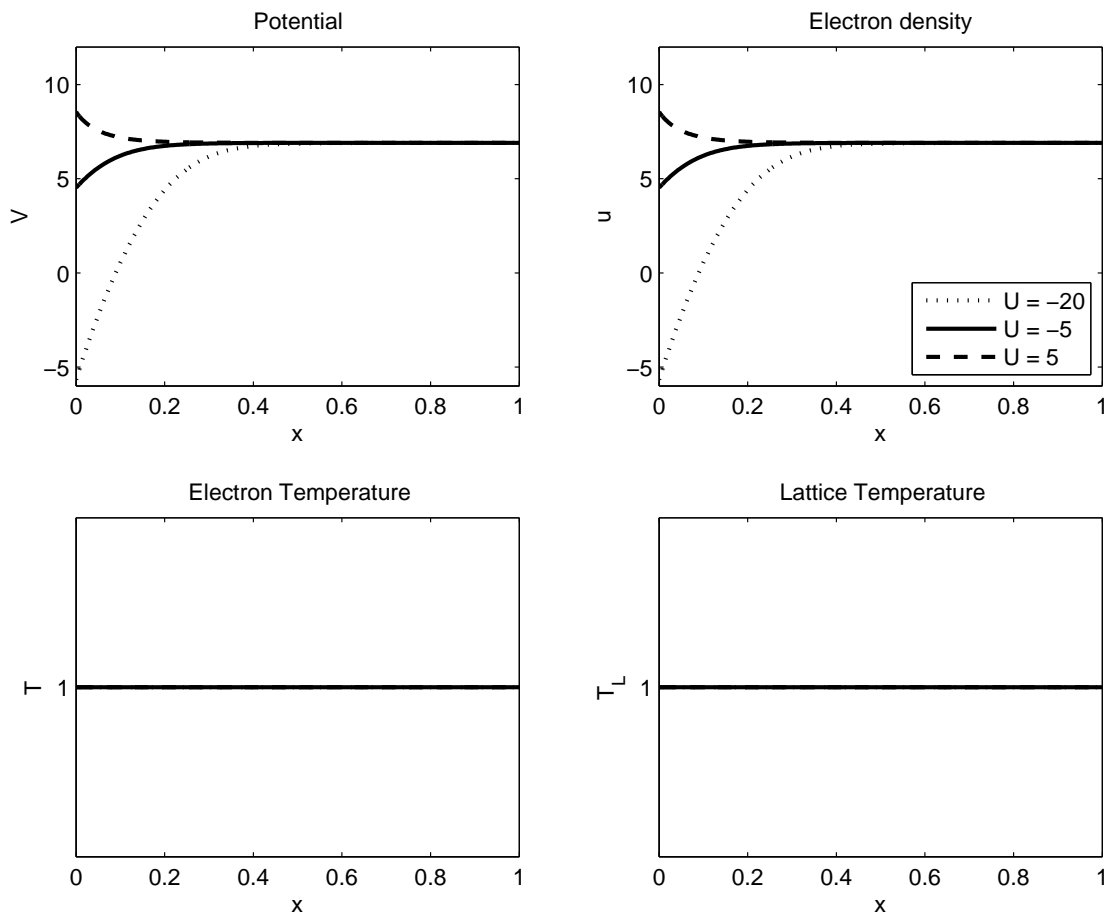


FIGURE 4. State variables for various applied voltages ( $T_0 = T_1 = 1$ ). The electron density is depicted in logarithmic scale.

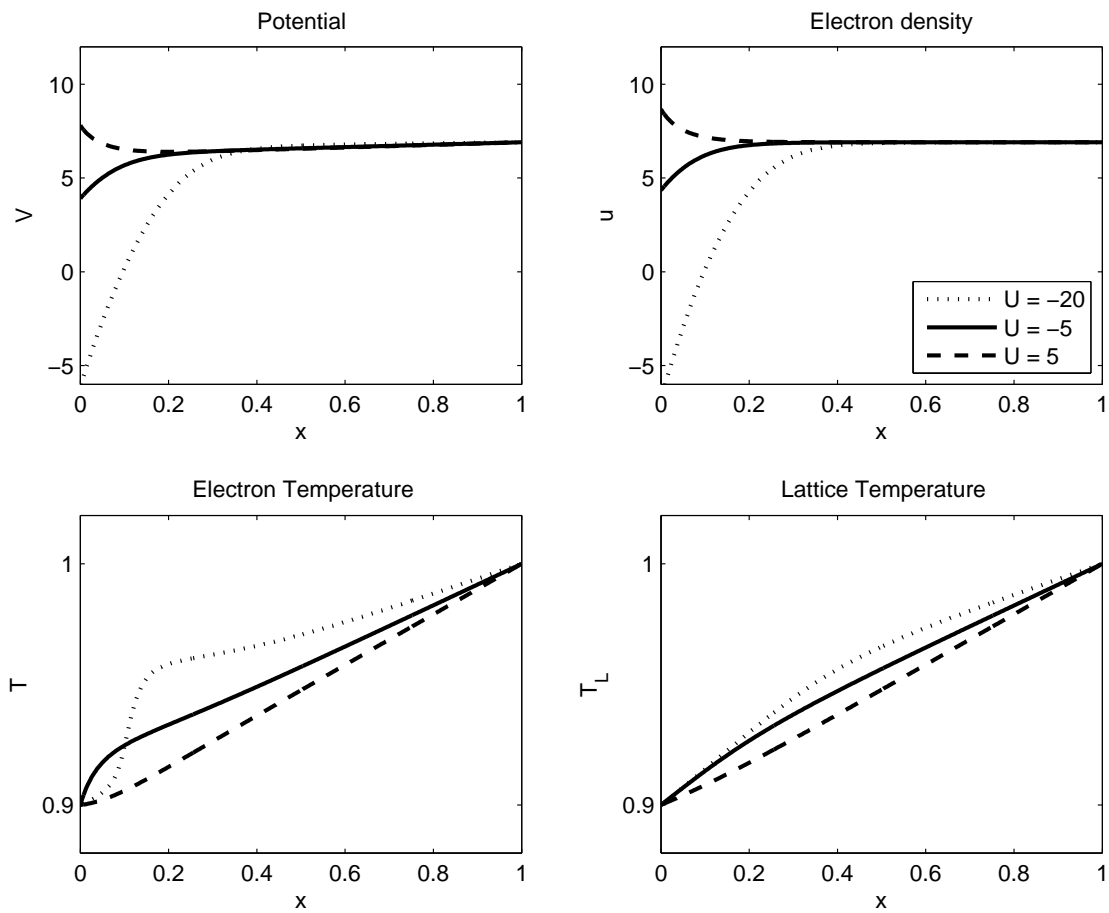


FIGURE 5. State variables for applied different voltages ( $T_0 = 0.9$ ). The electron density is depicted in logarithmic scale.